Available online at www.sciencedirect.com
SCIENCE DIRECT®
Journal of Photochemistry and Photobiology A: Chemistry 162 (2004) 253–259
Journal of Photochemistry and Photobiology A:Chemistry
www.elsevier.com/locate/jphotochem

Light-driven oxygen scavenging by titania/polymer nanocomposite films

Li Xiao-e[a,b], Alex N.M. Green[a], Saif A. Haque[a], Andrew Mills[c], James R. Durrant[a,*]

[a] *Centre for Electronic Materials and Devices, Department of Chemistry, Imperial College London, London SW7 2AZ, UK*
[b] *College of Chemical Engineering, Northwest University, Xi'an 710069, PR China*
[c] *Department of Pure and Applied Chemistry, University of Strathclyde, Glasgow G1 1XL, UK*

Received 17 July 2003; received in revised form 17 July 2003; accepted 26 August 2003

Abstract

We demonstrate that UV illumination of nanocrystalline TiO_2 films in the presence of excess organic hole scavengers can result in the deoxygenation of a closed environment. The kinetics of deoxygenation are investigated under continuous UV illumination as a function of film preparation and hole scavenger employed. Optimum deoxygenation is observed using methanol as a hole scavenger, although efficient deoxygenation is also observed for a range of different polymer/TiO_2 nanocomposite films deposited on glass and plastic substrates. Transient absorption spectroscopy is used to probe the kinetics of the deoxygenation reaction, focusing on the kinetics of the reduction of oxygen by photogenerated TiO_2 electrons. Under aerobic conditions, this oxygen reduction reaction is observed to exhibit first order kinetics with a rate constant of $70\,s^{-1}$, more than one order of magnitude faster than alternative reaction pathways for the photogenerated electrons. These observations are discussed in terms of the Langmuir–Hinshelwood equation for photocatalytic action.

Keywords: Oxygen scavenging; Photocatalysis; Nanocrystalline TiO_2; Polymer

1. Introduction

Heterogeneous photocatalysis is attracting extensive interest for the degradation of organic pollutants [1–13]. Attention has particularly focused on the photocatalytic activity of nanocrystalline TiO_2 powders or films under ultraviolet illumination. This photocatalytic activity can be summarised as follows:

$$\text{Organic} + O_2 \xrightarrow[TiO_2]{h\nu \geq 3.2\ \text{eV}} CO_2 + H_2O \quad (1)$$

In this reaction, UV illumination results in the photogeneration of electrons and holes pairs in respectively the conduction and valence band of the TiO_2. Photogenerated holes can react with surface hydroxyl groups to generate surface absorbed hydroxyl radicals ($TiOH^{\bullet+}$) that, in turn, can oxidise the pollutant to its mineral form. Photogenerated electrons reduce absorbed oxygen to generate superoxide ions ($O_2^{\bullet-}$), which can be subsequently reduced to hydrogen peroxide (H_2O_2) and then water. The intermediate species produced can act as a further source of hydroxyl radicals ($OH^{\bullet}$) [1]. Both holes and $OH^{\bullet}$ are highly reactive in achieving the photoxidation of organic compounds [14–20].

The efficiency of the photocatalytic reaction is strongly dependent upon the presence of molecular oxygen. The reaction of molecular oxygen with the photogenerated electrons is for example thought to be essential in preventing charge recombination of the photogenerated electrons and holes within the TiO_2 nanoparticles. It has been found that photocatalytic activity of TiO_2 nanoparticles is nearly completely suppressed in the absence of oxygen, and that the steady-state concentration of oxygen has a profound effect on the rate of photocatalysed decomposition of organic compounds [21,22].

A consequence of the photocatalytic activity expressed in Eq. (1) is the consumption of molecular oxygen. In this paper, we focus upon this oxygen scavenging effect of the photocatalytic process. This consumption has been reported previously [13,21], but has not previously been considered in detail, and its technological significance has not been widely considered. We note that the achievement of anaerobic environments is a key issue in a wide range of applications, ranging from food packaging to organic electronics. The development of an efficient light driven oxygen scavenging system would be novel approach to achieving such anaerobic environments.

* Corresponding author. Tel.: +44-20-7594-5321; fax: +44-20-7594-5801.
E-mail address: j.durrant@ic.ac.uk (J.R. Durrant).

1010-6030/$ – see front matter © 2004 Elsevier B.V. All rights reserved.
doi:10.1016/j.nainr.2003.08.010

In order to focus on the oxygen dependence of the photocatalytic activity, the study we present herein employs UV excitation of nanocrystalline TiO_2 films in the presence of excess organic electron donor ('sacrificial' electron donor or 'SED'). The presence of excess organic allows us to focus on the oxygen dependence of the reaction mechanism, and to address the ability of such films to achieve the light driven deoxygenation of closed environments. Three issues are addressed. First of all, we consider the light driven oxygen scavenging efficiency of such films, focusing in particular on solid polymer/TiO_2 nanocomposite films due to their attractiveness for technological applications. Secondly, we employ transient laser spectroscopy to study the reaction of photogenerated electrons with molecular oxygen. In this regard, we exploit the optical transparency of the nanocrystalline TiO_2 films employed in this study, facilitating the use of transient absorption spectroscopy to probe the reaction mechanism. Finally, we fit these data in terms of a kinetic model, and demonstrate that these data are consistent with the functional form of the Langmuir–Hinshelwood equation.

2. Experimental

All chemicals used were obtained from Sigma–Aldrich or their subsidiaries, unless otherwise stated.

2.1. TiO_2 paste preparation

Films fabricated from two types of TiO_2 nanoparticles were studied: Degussa P25 and nanocrystalline TiO_2 particles (nc-TiO_2) synthesised by the aqueous hydrolysis of titanium isopropoxide.

2.1.1. P25 paste preparation

Three grams P25 Degussa was ground in a mortar and pestle along with 1 ml water and 0.1 ml acetylacetone. The suspension was slowly diluted under continuous grinding with 4 ml of water and then 0.05 ml of Triton X100 was added [23].

2.1.2. nc-TiO_2 paste preparation

Twenty-five millilitres of titanium isopropoxide was injected into 5.5 g of glacial acetic acid under argon and stirred for 10 min. The mixture was then injected into 120 ml of rapidly stirred 0.1 M nitric acid in a conical flask. The flask was left uncovered and heated at 80 °C for 8 h. After cooling, the solution was diluted to 5 wt.% TiO_2, and then autoclaved at 220 °C for 12 h. To ensure re-dispersal of the colloids, a 60 s full power burst from a LDU Soniprobe sonic horn was applied. The solution was then concentrated using a rotary evaporator and membrane vacuum pump. The resulting colloidal suspension comprised 12.5% (w/v) 10–15 nm diameter, anatase TiO_2 particles, as we have reported previously [24].

2.2. Film deposition

The resulting P25 and nc-TiO_2 aqueous pastes were deposited on glass microscope slides and plastic (acetate) substrates. Pastes were deposited either with or without the prior addition of organic SEDs. Organic SEDs added (50% mass relative to TiO_2) were carbowax (molecular mass: 20,000), poly-(vinyl chloride) (PVC, M_n ca. 5.5×10^4), polyethylene glycol (PEG, M_n ca. 1500) and polyethylene oxide (PEO, M_v ca. 4×10^6). All pastes were stirred slowly overnight prior to film deposition to ensure homogeneity and that no air bubbles were trapped within them. Further experiments employed methanol, PVC and PEG as SEDs added to the films following film deposition.

Pastes were deposited by the doctor blade method and allowed to dry in air for 20 min. Following film drying, two alternative post-treatments were employed. nc-TiO_2 deposited on glass substrates with carbowax were studied with and without employing a high-temperature sintering at 450 °C for 20 min (nc-TiO_2-HT and nc-TiO_2/carbowax films, respectively). P25 films deposited on plastic with PEG were studied with and without employing compression under high pressure 1×10^4 kg/cm^2 (P25/PEG-HP and P25/PEG films, respectively). Following the deposition post-treatments (nc-TiO_2-HT and P25/PEG-HP films), film thicknesses were determined to be 4 μm, with film thicknesses in the absence of post-treatments being estimated as approximately two times thicker, depending upon the film composition. Following film preparation, all films were cut into 1 cm^2 pieces for characterisation.

2.3. Oxygen scavenging measurements

Oxygen concentration measurements were made with an oxygen measurement electrode (Rank Brothers Ltd., Cambridge, UK). Films were inserted in a home built photoelectrochemical cell (cell volume: ∼0.5 cm^3), and the oxygen concentration of the cell monitored as a function of illumination time. A UV 365 nm lamp was used as the irradiation source (VL-208BL, intensity: 1400 μW/cm^2).

2.4. Transient absorption data

Transient optical studies employed nc-TiO_2-HT fabricated as detailed above on TCO glass substrates, selected due to their minimal light scattering properties. Films were studied in the 'sandwich cell' configuration with a surlyn 1472 seal (Dupont Ltd.). Following fabrication, the cell was filled with acetonitrile dried with molecular sieves and bubbled with argon for 30 min with and without the addition of 10% methanol as SED. Cells were studied both fully sealed, and with the acetonitrile insertion holes left unsealed.

Transient absorption data were conducted as reported previously [25], employing a PTI GL-3300 nitrogen laser (337 nm, 30 μJ cm^{-2}, 0.8–4 Hz) as excitation source.

3. Results

3.1. Electrochemical analysis of oxygen scavenging

We consider first the ability of the TiO_2/SED film to scavenge molecular oxygen from a sealed oxygen electrode cell. The experimental procedure involved the use of the oxygen electrode to monitor the gaseous oxygen concentration of the cell as a function of UV illumination time. Typical data are shown in Fig. 1, showing data collected with nc-TiO_2 films fabricated on glass slides without any heat post-treatment as a function of SED employed. Control data with nc-TiO_2 films in the absence of any SED, and for a SED (methanol) in the absence of nc-TiO_2, showed comparatively negligible oxygen scavenging function (traces a) and b)). Traces c–f compare nc-TiO_2 films with four different SEDs: methanol, PVC, PEG and PEO. Strong oxygen scavenging function is observed for all films. It is apparent that methanol functions as the most efficient SED. The three polymers were all blended with the nc-TiO_2 paste prior to film deposition, and then co-deposited, with PVC proving to be most efficient polymer SED. An alternative methodology, depositing the nc-TiO_2 film alone, and then spin coating the polymer onto this film (trace g) gave significantly reduced oxygen scavenging activity, most probably due to poor penetration of the polymer into the film pores.

We turn now to comparison of different TiO_2 preparations and post-treatments. Typical data are shown in Fig. 2 for three different film fabrication routes. UV-Vis (1-transmission) spectra for these three films are shown in Fig. 3. As the optical bandgap for all three films lies in the ultraviolet, the differences in visible light transmission between these films is attributed primarily to their different light scattering properties. Films fabricated from the nc-TiO_2 were non-scattering, independent of film post-treatment or blending with polymer (trace a). Films fabricated from the P25 were strongly scattering and opaque (trace c). The high-pressure post-treatment resulted in a significant reduction in the scattering properties of the films, as shown in Fig. 3 (trace b). Comparison of Figs. 2 and 3 demonstrates that there is a correlation between the optical transparency of the film and its oxygen scavenging activity, with films which exhibited the lowest light scattering exhibiting the highest activity. This correlation was found to be independent of SED employed, with similar trends being observed using methanol as a SED (data not shown).

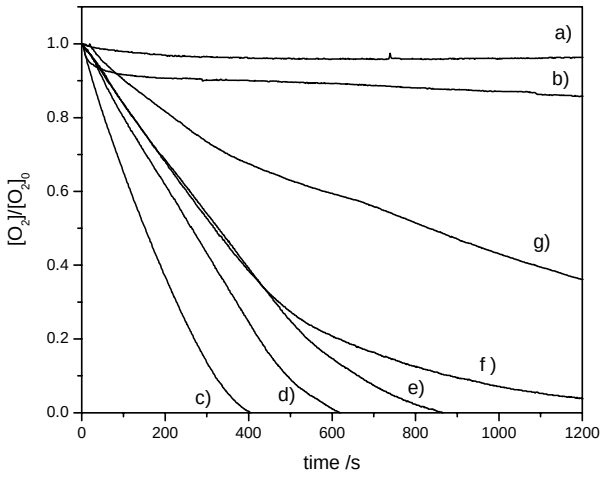

Fig. 1. Dependence of oxygen scavenging activity on sacrificial electron donor. Data are shown as the normalised oxygen concentration as a function of UV irradiation time in a closed cell employing the following photoactive films deposited on glass slides: (a) nc-TiO_2 only; (b) MeOH only; (c) nc-TiO_2/MeOH; (d) nc-TiO_2/PVC (co-deposited); (e) nc-TiO_2/PEG (co-deposited); (f) nc-TiO_2/PEO (co-deposited); and (g) nc-TiO_2/PVC (post-addition).

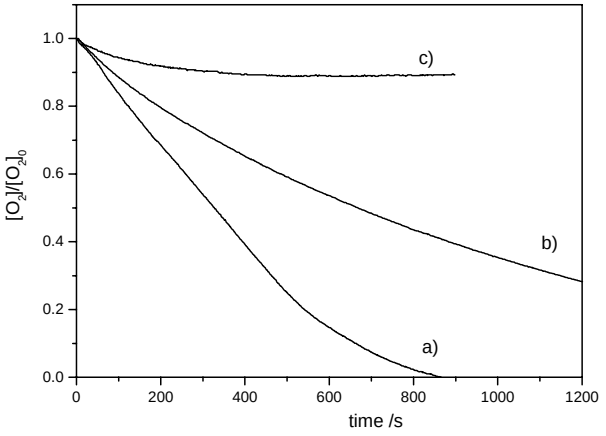

Fig. 2. Dependence of oxygen scavenging activity of TiO_2/PEG nanocomposite films for three different film fabrication procedures: (a) nc-TiO_2/PEG film on glass microscope slide without high pressure; (b) P25/PEG-HP film on plastic with high pressure; and (c) P25/PEG film on plastic without high pressure. Data are shown as the normalised oxygen concentration as a function of UV irradiation time in a closed cell.

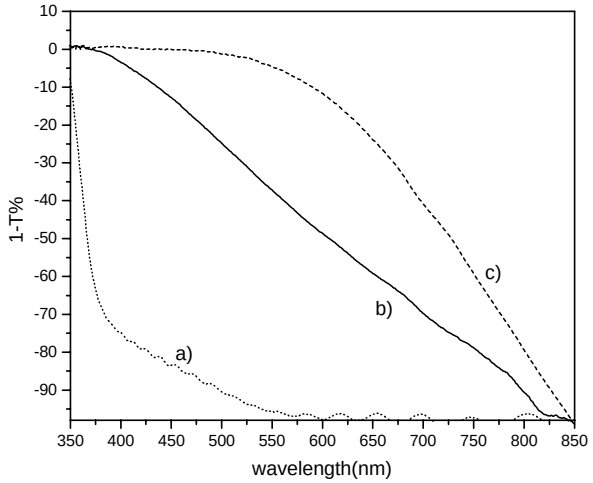

Fig. 3. (1-Transmission) spectra of TiO_2/PEG nanocomposite films for three different film fabrication procedures: (a) nc-TiO_2/PEG film on glass microscope slide without high pressure; (b) P25/PEG-HP film on plastic with high pressure; and (c) P25/PEG film on plastic without high pressure.

In addition to reducing the light scattering properties of the nanocomposite films, the high-pressure post-treatment employed in trace b of Figs. 2 and 3 has been shown to improve the electrical connectivity of the TiO_2 nanoparticles by sintering the particles together [26]. In order to evaluate whether such improved connectivity could influence the oxygen scavenging activity of the films, further experiments were conducted using the alternative high-temperature post-treatment, a procedure which has also been shown to improve the connectivity between particles. However, in contrast to the high-pressure post-treatment, this high-temperature post-treatment was found to reduce the oxygen scavenging activity of the films (data not shown). We conclude that the oxygen scavenging activity is not enhanced (and may actually be reduced) by improved electrical connectivity of the TiO_2 nanoparticles. We note that the reduced activity following the heat treatment may also be associated with sodium diffusion from the glass substrate into the TiO_2 film. The improved activity observed following the high-pressure post-treatment is attributed to the reduced optical light scattering of the film. This dependence upon light scattering can be most reasonably be attributed to improved penetration of the 365 nm excitation light into the non-scattering films.

3.2. Transient absorption studies of oxygen reduction

The photocatalytic reaction detailed in Eq. (1), which is the basis of the oxygen scavenging process reported here, has a complex reaction mechanism. Transient absorption spectroscopy has been used previously to interrogate the reactive intermediates in this reaction. In particular, it has been shown that the induced absorption of photogenerated electrons and holes within the TiO_2 nanocrystals can be used to monitor the generation and decay dynamics of these species [27]. The electrochemical data presented above address the overall rate of light driven oxygen scavenging as a function of oxygen concentration. A full transient absorption study of all the reactive intermediates in this oxygen scavenging process is beyond the scope of this paper. We focus here rather on a key step in the oxygen consumption process, the reduction of molecular oxygen by electrons photogenerated in the TiO_2 nanoparticles.

The experimental procedure involved the pulsed UV excitation of nc-TiO_2-HT films in the presence and absence of oxygen, employing methanol dissolved in acetonitrile as a SED. Fig. 4 shows the kinetics of the transient absorption signal monitored at 800 nm in the presence and absence of methanol, collected under anaerobic conditions. In the absence of methanol, a photoinduced absorption transient is observed which exhibits a rapid decay time (half-life of $<30\ \mu s$). We attribute this rapid decay time to recombination of photogenerated electrons and holes within the TiO_2 film, consistent with previous observations [28]. In the presence of methanol, a large amplitude, long-lived signal is observed (half-life of $\sim$500 ms). We attribute this signal to long lived

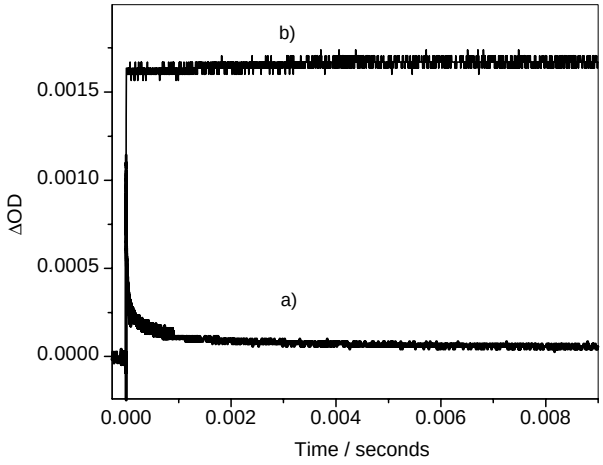

Fig. 4. (a) Transient absorption data for a nc-TiO_2-HT film in an anaerobic sealed cell in the absence (trace a) and presence (trace b) of methanol SED. Data were collected at a probe wavelength of 800 nm, following pulsed excitation at 337 nm (repetition rate: 0.8 Hz).

electrons in the TiO_2 derived from the removal of holes by the methanol hole scavenger. This observation is consistent with previous studies by Bahnemann et al. [27]. The transient absorption spectrum of this long lived signal (presented elsewhere [29]) exhibited a broad absorption increase in the red/near infrared, with a maximum around 680 nm, consistent with the assignment of this signal to long lived electrons in the TiO_2 [27].

Fig. 5 compares the transient absorption signal in the presence of methanol, but under aerobic (trace a) or anaerobic conditions (trace b). Data are presented with a logarithmic time axis to facilitate comparison of the two traces. It is apparent that the presence of oxygen results in an acceleration of the decay of the transient signal to $\sim$10 ms, a 50-fold acceleration relative to the anaerobic data. This acceleration

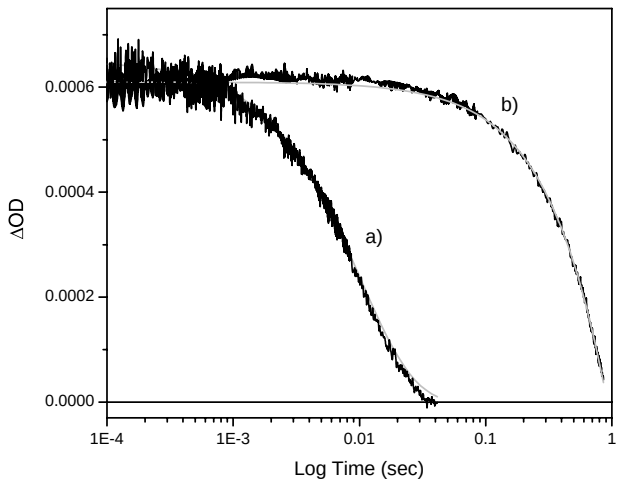

Fig. 5. Transient absorption data for a nc-TiO_2-HT film in the presence of methanol SED in an unsealed, and therefore aerobic, cell (trace a) and a sealed, anaerobic cell (trace b). Other experimental conditions as in Fig. 4. Smooth grey lines correspond to monoexponential fits to the transient decays.

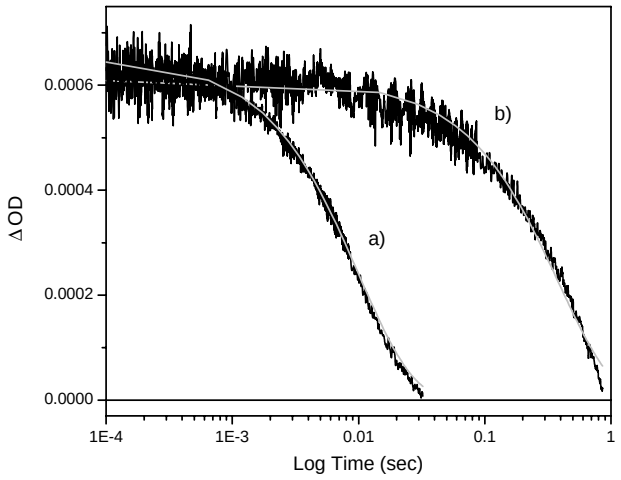

Fig. 6. Transient absorption data for a nc-TiO_2-HT film in an unsealed cell in the presence of methanol SED as a function of repetition rate of the UV excitation pulses: trace (a) 0.8 Hz and trace (b) 4 Hz. Other experimental conditions as in Fig. 4. Smooth grey lines correspond to monoexponential fits to the transient decays.

is assigned to the well known reaction of photogenerated electrons with molecular oxygen [27,30], resulting in the generation of the $O_2^{\bullet -}$. Also shown in Fig. 5 (smooth, grey lines) are first order, monoexponential fits to the transient decays, showing excellent agreement with the experimental data, yielding first order rate constants for the transients of 70 and 1.4 s^{-1} under aerobic and anaerobic conditions, respectively.

Fig. 6 presents further data in support of the oxygen scavenging activity of the TiO_2 film. Data were collected in the presence of methanol in an unsealed cell, as for trace a of Fig. 5, as a function of the repetition rate of the excitation laser pulses. Trace a corresponds to 0.8 Hz repetition rate, as employed in Figs. 4 and 5. Trace b in Fig. 6 corresponds to a faster repetition rate of 4 Hz, and was collected after prolonged excitation of the sample. It is apparent that the faster repetition rate results in an ~40-fold retardation of the decay dynamics of the transient signal. This retardation was fully reversible after allowing the system to equilibrate again at the lower repetition rate. The retardation of the signal decay at high repetition rate is consistent with deoxygenation of the cell by the pulsed UV excitation, with the rate of oxygen consumption exceeding the rate of oxygen diffusion into the cell, and provides further evidence for the oxygen scavenging ability of the nanocrystalline TiO_2 films in the presence of excess SED.

4. Discussion

4.1. Demonstration of light driven deoxygenation of a closed environment

The data we present here clearly demonstrate that UV illumination of a nanocrystalline TiO_2 film in the presence of excess sacrificial electron donor can result in the deoxygenation of a closed environment. The rate of oxygen consumption (the gradients of graphs 1 and 2) is only weakly dependent upon oxygen concentration, resulting in efficient oxygen consumption even at low oxygen concentrations, and leading to essentially complete deoxygenation (final oxygen concentration <0.02%).

The rate of oxygen consumption is found to be dependent upon materials employed. Oxygen consumption is found to be favoured by the use of a non-scattering TiO_2 film, attributed to improved penetration of the UV light into the film. Of particular technological significance, we demonstrate that polymer/TiO_2 nanocomposite films deposited on plastic substrates exhibit strong oxygen scavenging activity. Optimum activity of such films requires co-deposition of the TiO_2 nanoparticles and polymer to ensure an intimate mixing of the two components, followed by a high-pressure compression step to minimise light scattering by the deposited film. PEO, PEG and PVC all functioned as SEDs in polymer/TiO_2 nanocomposite films. PVC exhibited the highest activity, although environmental concerns indicate that PEO and PEG may be more suitable for practical applications.

4.2. Transient absorption dynamics

The key reaction steps associated with oxygen consumption can be summarised by the following equations:

$$TiO_2 + h\nu \rightarrow e^- + h^+ \quad (2)$$

$$e^- + h^+ \xrightarrow{r_3} TiO_2 \quad (3)$$

$$h^+ + SED \xrightarrow{r_4} SED^+ \quad (4)$$

$$e^- + O_2 \xrightarrow{r_5} O_2^{\bullet -} \quad (5)$$

$$e^- + Q \xrightarrow{r_6} Q^- \quad (6)$$

where Q is any electron acceptor species distinct from molecular oxygen and r_i is the rate of reaction i under the experimental conditions studied. We note that the quenching species Q in Eq. (6) are likely to be primarily oxidised SED (SED^+), resulting in the absence of oxygen in no net photocatalytic activity, consistent with experimental observations.

The transient absorption data shown in Figs. 4–6 give us clear indications of the rates of several of these reactions, at least for the example of a nanocrystalline TiO_2/SED film studied. Fig. 4 showing data for a nanocrystalline TiO_2 in the absence of SEDs gives a half time for reaction 3 of $\ll$30 μs, corresponding to $r_3 > 10^5\ s^{-1}$. The addition of methanol to the film results in reaction 4, hole scavenging by the SED, competing effectively with the recombination reaction. It can be concluded that for this experimental system, $r_4 \gg r_3$. In the absence of oxygen, the half time of the photogenerated electrons is ~500 ms. The monoexponential fit to this decay

yields an effective first order rate constant for electron reaction with alternative electron acceptors Q, r_6 of $\sim 1.4\,s^{-1}$. In contrast, under aerobic conditions, the electron half time is reduced to ~10 ms, with monoexponential analysis yielding a value for the rate constant r_5 of $70\,s^{-1}$. Our observation that under aerobic conditions $r_5 \gg r_6$ indicates that the yield of the oxygen reduction reaction (reaction 5) will be rather insensitive to oxygen concentration over at least an order of magnitude reduction in oxygen concentration. This conclusion is of particular importance for kinetic modelling of the oxygen consumption data, as we discuss below.

4.3. Kinetic model of oxygen consumption

The rate of photocatalytic destruction of organic pollutants by TiO_2, as described by reaction 1, is typically modelled by the Langmuir–Hinshelwood equation [19]. In the limit of excess organic sacrificial electron donor, this equation can be simplified to

$$r = \frac{A[O_2]}{1 + B[O_2]} \tag{7}$$

where r is the rate of consumption of organic material, and A and B are constants dependent upon the photocatalyst and experimental conditions employed. In order to compare with our experimental data, we make the assumption that the rate consumption of organic material is proportional to the rate of oxygen consumption.

Eq. (7) simplifies in the limits of high and low oxygen concentrations. In the limit of high oxygen concentration, $B[O_2] \gg 1$, Eq. (7) becomes

$$r = \frac{A}{B} = \text{constant} \tag{8}$$

and zeroth-order behaviour is expected with the oxygen concentration decaying linearly with time. In the limit of low oxygen concentration, $B[O_2] \ll 1$, and Eq. (7) becomes

$$r = A^*[O_2] \tag{9}$$

In this limit, a first order, exponential decay of oxygen concentration is expected.

Qualitatively, the experimental data shown in Figs. 1 and 2 are in good agreement with behaviour predicted by Eqs. (8) and (9). At early times, the oxygen concentration decays rather linearly with time. At low oxygen concentrations, deviations from linearity are observed consistent with more first order like behaviour.

More quantitatively, the experimental data were fitted to the integrated form of the rate law as given by Eq. (10):

$$t = \frac{B[O_2]_0}{A'}\left(1 - \frac{[O_2]}{[O_2]_0}\right) - \frac{1}{A'}\ln\frac{[O_2]}{[O_2]_0} \tag{10}$$

Typical fits are shown in Fig. 7. Given that the fitting includes only two variable parameters, A and B, the fits are in excellent agreement with the experimental data.

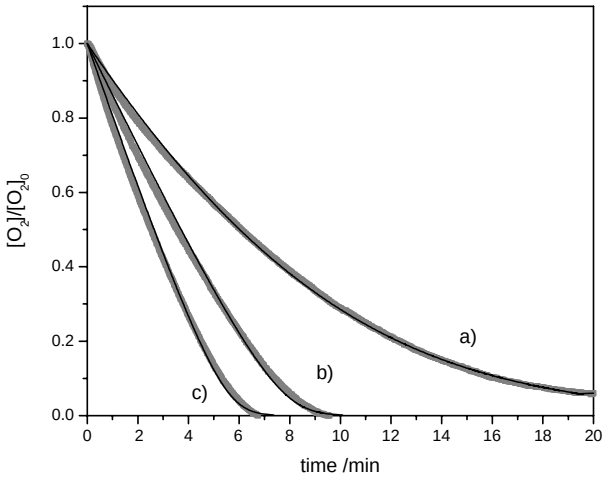

Fig. 7. Comparison between experimental observations of light driven oxygen consumption (gray lines) against the theoretical integrated rate law, Eq. (10) (black lines). Traces are shown for three different TiO_2 films, all deposited on glass and employing MeOH added as SED: (a) P25; (b) nc-TiO_2/carbowax; and (c) nc-TiO_2.

We note that an assumption inherent in the derivation of Eqs. (7)–(10) is that the rate of oxygen consumption reaction, and therefore the quantum yield of oxygen photoreduction (Eq. (5)) is proportional to concentration of surface bound oxygen. The transient optical data presented in Figs. 4–6 question the validity of this assumption in the presence of excess SED. Under these conditions, the yield of hole scavenging by the SED is essentially unity, and the yield of oxygen reduction will depend only upon the kinetic competition between oxygen reduction (Eq. (5)) and the quenching/recombination reaction (Eq. (6)):

$$\Phi(O_2^{\bullet -}) = \frac{r_5}{(r_5 + r_6)} \tag{11}$$

r_5 is expected to be dependent upon oxygen coverage of the photocatalyst, whilst r_6 should be independent of oxygen coverage. The transient absorption data shown in Figs. 5 and 6 indicate that the rate of reaction 5 in the presence of oxygen ($70\,s^{-1}$) is fast compared to reaction 6 ($1.4\,s^{-1}$)—i.e. $r_5 \gg r_6$. In this limit, the yield of oxygen reduction will be rather insensitive to r_5 and therefore the oxygen coverage on the TiO_2 surface (except at very low oxygen concentrations), in contrast to the assumption given above. We note however that this issue does not change the functional form of Eq. (7), and therefore the validity of the fits shown in Fig. 7, but only the definitions of the constants A and B. Further, more quantitative consideration of this issue will be presented elsewhere.

The experimental data shown in Figs. 1 and 2 clearly demonstrate that the oxygen scavenging kinetics are dependent upon the TiO_2 film preparation and organic hole scavenger employed. This dependence can be attributed in part to difference in optical scattering between the films, as illustrated in Fig. 3. Further differences are likely to derive from difference in the rates of the underlying reaction steps,

such as those indicated in Eqs. (3)–(6). Transient absorption experiments to address this issue are currently in progress.

Acknowledgements

Financial support from the EPSRC is gratefully acknowledged. We also thank the China Shannxi Science and Technology Committee and China Scholarship Committee (CSC) for supporting this work through the award of a fellowship to XL, and Emilio Palomares, Ana Peiro Munoz and Jenny Nelson for helpful discussions.

References

[1] A. Mills, S. Lee, A web-based overview of semiconductor photochemistry-based current commercial applications, J. Photochem. Photobiol. A: Chem. 152 (2002) 233–247.
[2] I.M. Arabatzis, S. Antonaraki, T. Stergiopoulos, et al., Preparation, characterization and photocatalytic activity of nanocrystalline thin film TiO_2 catalysts towards 3,5-dichlorophenol degradation, J. Photochem. Photobiol. A: Chem. 5929 (2002) 1–9.
[3] S.B. Kim, S.C. hong, Kinetic study for photocatalytic degradation of volatile organic compounds in air using thin film TiO_2 photocatalyst, Appl. Catal. B: Environ. 35 (2002) 305–315.
[4] Y. Hsien, C. Chang, Y. Chen, et al., Photodegradation of aromatic pollutants in water over TiO_2 supported on molecular sieves, Appl. Catal. B: Environ. 31 (2001) 241–249.
[5] M. Rosana, W. Alberici, F. Jardim, Photo catalytic destruction of VOCs in the gas-phase using titanium dioxide, Appl. Catal. B: Environ. 14 (1997) 55–68.
[6] T. Minabe, D.A. Tryk, P. Sawunyama, et al., TiO_2-mediated photodegradation of liquid and solid organic compounds, J. Photochem. Photobiol. A: Chem. 137 (2002) 53–62.
[7] D.V. Kozlov, E.A. Paukshtis, E.N. Savinov, The comparative studies of titanium dioxide in gas-phase ethanol photocatalytic oxidation by the FTIR in situ method, Appl. Catal. B: Environ. 24 (2000) L7–L12.
[8] K. Vinodgopal, V. Kamat, Electrochemically assisted photocatalysis using nanocrystalline semiconductor thin films, Sol. Energy Mater. Sol. Cells 38 (1995) 401–410.
[9] L. Su, Z. Lu, Spectroelectrochemical study of TiO_2 particulate films, Spectrochim. Acta Part A 53 (1997) 1719–1722.
[10] A. Mills, N. Elliott, I.P. Parkin, et al., Novel TiO_2 CVD films for semiconductor photocatalysis, J. Photochem. Photobiol. A: Chem. 151 (2002) 171–179.
[11] M.R. Hoffmann, S.T. Martin, W. Choi, et al., Environmental applications of semiconductor photocatalysis, Chem. Rev. 95 (1995) 69–96.
[12] A. Heller, Chemistry and applications of photocatalytic oxidation of thin organic films, Acc. Chem. Res. 28 (1995) 503–508.
[13] A.L. Linsebigler, G. Lu, J.T. Yates Jr., Photocatalysis on TiO_2 surfaces: principles, mechanisms, and selected results, Chem. Rev. 95 (1995) 735–758.
[14] U. Gesenhues, Influence of titanium dioxide pigments on the photodegradation of poly(vinyl chloride), PVC Degrad. Stab. 68 (2000) 185–196.
[15] S. Cho, W. Choi, Solid-phase photocatalytic degradation of PVC-TiO_2 polymer composites, J. Photochem. Photobiol. A: Chem. 143 (2001) 121–228.
[16] S. Horikoshi, N. Serpone, Y. Hisamatsu, et al., Photocatalyzed degradation of PVCs in aqueous semiconductor suspensions. 3. Photooxidation of a solid PVC: TiO_2-blended poly(vinyl chloride) film, Environ. Sci. Technol. 32 (1998) 4010–4016.
[17] H. Uchida, S. Katoh, M. Watanabe, Photocatalytic degradation of trichlorobenzene using immobilized TiO_2 films containing poly(tetrafluoroethylene) and platinum metal catalyst, Electrochim. Acta 43 (14–15) (1998) 2111–2116.
[18] K. Hasegawa, C. Wen, T. Kotani, et al., Photocatalyzed degradation of agrochemicals using poly(2,5-dihexoxy-*p*-phenylene) and poly(3-octylthiophene-2,5-diyl) films, J. Mater. Sci. Lett. 18 (1999) 1091–1093.
[19] A. Mills, J. Wang, Photomineralisation of 4-chlorophenol sensitized by TiO_2 thin films, J. Photochem. Photobiol. A: Chem. 118 (1998) 53–63.
[20] Y. Kotani, T. Matada, A. Matsudo, et al., Anatase nanocrystal-dispersed thin fims via sol-gel process with hot water treatment: effect of poly(ethylene glycol) addition on photocatalytic activities of the films, J. Mater. Chem. 11 (2001) 2045–2048.
[21] J. Herrmann, Active agents in Heterogeneous Photocatalysis: Atomic Oxygen Species vs. OH·Radicals: Related Quantum Yields, Helvetica Chim. Acta 84 (2001) 2731–2750.
[22] K. Ishibashi, A. Fujishima, T. Watanabe, et al., Detection of active oxidative species in TiO_2 photocatalysis using the fluorescence technique, Electrochem. Commun. 2 (2002) 207–210.
[23] K. Ladislav, B. O'Regan, K. Andreas, M. Graetzel, Preparation of TiO_2 (anatase) films on electrodes by anodic oxidative hydrolysis of TiO_3, J. Electroanal. Chem. 346 (1993) 291.
[24] R.L. Willis, C. Olson, B. O'Regan, et al., Electron dynamics in nanocrystalline ZnO and TiO_2 films probed by potential step chronoamperometry and transient absorption spectroscopy, J. Phys. Chem. B 106 (2002) 7605–7613.
[25] S.A. Haque, et al., Parameters influencing charge recombination kinetics in dye-sensitised nanocrystalline titanium dioxide films, J. Phys. Chem. B 104 (2000) 538.
[26] H. Lindstrom, A. Holmberg, E. Magnusson, S.E. Lindquist, L. Malmqvist, A. Hagfeldt, A new method for manufacturing nanostructured electrodes on plastic substrates, Nano Lett. 1 (2) (2001) 97.
[27] D. Bahnemann, A. Henglein, J. Lillie, L. Spanhel, Flash photolysis observation of the absorption spectra of trapped positive holes and electrons in colloidal TiO_2, J. Phys. Chem. 88 (1984) 709.
[28] J. Rabani, K. Yamashita, K. Ushida, J. Stark, A. Kira, Fundamental reactions in illuminated titanium dioxide nanocrystallite layers studied by pulsed laser, J. Phys. Chem. B 1689 (1998) 102.
[29] A.N.M. Green, R. Chandler, S.A. Haque, J. Nelson, J.R. Durrant, manuscript in preparation.
[30] J. Nelson, A.M. Eppler, I.M. Ballard, Photoconductivity and charge trapping in porous nanocrystalline titanium dioxide, J. Photochem. Photobiol., A: Chem. 148 (1–3) (2002) 25–31.